IJE TRANSACTIONS A: Basics Vol. 34, No. 7, (July 2021) 1586-1601

International Journal of Engineering

Journal Homepage: www.ije.ir

Straightforward Prediction for Responses of the Concrete Shear Wall Buildings Subject to Ground Motions Using Machine Learning Algorithms

M. S. Barkhordari*[a], M. S. Es-haghi[b]

[a] *Department of Civil and Environmental Engineering, Amirkabir University of Technology, Tehran, Iran*
[b] *School of Civil Engineering, Khajeh Nasir Toosi University of Technology, Tehran, Iran*

P A P E R I N F O

Paper history:
Received 16 April 2021
Received in revised form 18 May 2021
Accepted 19 May 2021

Keywords:
Artificial Neural Networks
Regression Model
Tall Buildings
Seismic Response

A B S T R A C T

The prediction of responses of the reinforced concrete shear walls subject to strong ground motions is critical in designing, assessing, and deciding the recovery strategies. This study evaluates the ability of regression models and a hybrid technique (ANN-SA model), the Artificial Neural Network (ANN), and Simulated Annealing (SA), to predict responses of the reinforced concrete shear walls subject to strong ground motions. To this end, four buildings (15, 20, 25, and 30-story) with concrete shear walls were analyzed in OpenSees.150 seismic records are used to generate a comprehensive database of input (characteristics of records) and output (responses). The maximum acceleration, maximum velocity, and earthquake characteristics are used as predictors. Different machine learning models are used, and the accuracy of the models in identifying the responses of the shear walls is compared. The sensitivity of input variables to the seismic demand model is investigated. It has been seen from the results that the ANN-SA model has reasonable accuracy in the prediction.

***doi**: 10.5829/ije.2021.34.07a.04*

NOMENCLATURE

T	Control variable	q	Probability of accepting the potential solution
ΔE_c	Changes in the value of the objective function	K_B	Boltzmann constant
y_i	i[th] value of the variable to be predicted	$\bar{y}$	Average ofy_i
$\hat{y}_i$	predicted value ofy_i		

1. INTRODUCTION

Reinforced concrete (RC) shear walls are efficient members for providing resisting horizontal forces in tall buildings. The non-linear analysis is needed to determine the tall buildings' seismic responses more realistically. However, non-linear modeling is a challenge for practitioner engineers because they should select the proper structural model type, define complex parameters of the materials, elements, and select as well as scale ground motions records. Besides, the ability to predict the structural capacity after an earthquake is essential to inform whether the tall building can be permanently reoccupied or not. Therefore, predicting the structure's response to a new earthquake based on the structure's response to past earthquakes could be an excellent solution to determine the extent of the damage. This is possible using machine learning techniques. In the last few years, research has been done on using machine learning in civil engineering [1-12]. For instance, Thaler et al. [2] developed a machine-learning-enhanced Monte Carlo simulation strategy to predict the structural response in earthquake engineering in which the neural networks are utilized to improve the reliability of the method in the tail end of the distribution. Stoffel et al. [10] developed an Artificial Neural Network accessible to complicated structural deformation under shock-wave loads. They calculated plate deflections by means of

*Corresponding Author Institutional Email: m.s.barkhordari@aut.ac.ir (M. S. Barkhordari)

Please cite this article as: M. S. Barkhordari, M. S. Es-haghi, Straightforward Prediction for Responses of the Concrete Shear Wall Buildings Subject to Ground Motions Using Machine Learning Algorithms, International Journal of Engineering, Transactions B: Applications, Vol. 34, No. 05, (2021) 1586-1601

finite element simulations including a neural network. Mangalathu and Jeon [7] applied machine learning techniques to identify the failure mode of beam-column joints. They also compared various machine learning techniques to estimate the shear strength of beam-column joints using an experimental database. Khaleghi et al. [13] have employed Artificial Neural Networks to predict load-bearing capacity and stiffness of perforated masonry walls. Mangalathu and Jeon [14] conducted a comparative study for failure mode recognition of RC bridge columns using various machine learning models. A clustering algorithm is proposed by Siam et al. [15] for structural performance classifications using a dataset of ninety-seven masonry shear walls. Kiani et al. [16] developed a method for deriving the fragility curves using various machine learning models. They also investigated the effect of training sample size and imbalanced dataset on machine learning models' performance. Gaba et al. [17] classified the damages caused by earthquakes using a previously acquired data set. To establish the best prediction model, they evaluated different machine learning classifier algorithms. Burton et al. [18] described a statistical approach to predict the aftershock collapse vulnerability of buildings. They also mentioned that the Kernel Ridge regression method produces the most accurate and stable predictions. Zhang et al. [19,20] utilized machine learning algorithms to link the capacity of damaged buildings to the response and damage patterns.

As mentioned above, Machine Learning methods to analyze and evaluate the dynamic characteristics of the structure have been studied in the literature. Nevertheless, few articles have focused on tall buildings, which are evaluated in the current paper. In addition, tall buildings have a large number of components and responses that lead to a high dimensional feature space, as opposed to low- or mid-rise buildings. Therefore, there is a need for a simple method to estimate the responses of the tall buildings subject to ground motion. In addition, a hybrid intelligent method, which is the optimization of the parameters in Artificial Neural Network by the revolutionary algorithm of Simulated Annealing, to achieve better performance for predicting the response of tall buildings.

In fact, This study's primary purpose is to evaluate the ability to exist simple machine learning methods and a hybrid technique (ANN-SA model), the Artificial Neural Network (ANN), and Simulated Annealing (SA) to estimate the responses of structures based on earthquake characteristics and the stored responses of a structure subjected to the earthquake. Specifically, the following objectives have been pursued throughout the research: (1) evaluating the performance of various machine learning models (namely linear regression, Ridge regression, Lasso regression, Elastic net regression, Huber regression, RANSAC, and ANN-SA model) in estimating of responses of high-rise-concrete-shear-wall buildings, (2) investigating the effectiveness of using maximum acceleration and maximum speed recorded by the sensor in predicting structural responses (3) identifying the significant input variables which influence the predicting the responses of tall buildings.

2. MATERIALS AND METHODS

The central assumption in this study is that there are sensors in the stories of the tall building so that the maximum acceleration or velocity in the tall building that is subjected to a new earthquake can be captured (these responses are recorded during the earthquake), and the building's responses such as drift, base shear, displacement, the maximum acceleration and velocity under previously recorded ground motions are calculated using any software (Database). In other words, we have the maximum velocity or acceleration in the building and the building's responses, such as the drift caused by previous earthquakes, and only the maximum acceleration and velocity, which created by the new earthquake, are recorded using sensors. Can this information be used to estimate the building's responses under the new earthquake? In order to evaluate this strategy, four buildings (15, 20, 25, and 30-story) with concrete shear walls were analyzed in OpenSees [21,22] to generate a dataset.

A percentage of total data is considered information obtained from the building subjected to the new earthquake (for example, 20%). This means that the obtained acceleration/velocity of this 20 % is considered the sensor's values under the new earthquakes, and the obtained responses (the maximum base shear, maximum drift, and maximum displacement) are considered as unknown variables. Therefore, the maximum acceleration, maximum velocity, and earthquake characteristics are used as predictors in order to estimate the maximum base shear, maximum drift, and maximum displacement for a specific seismic excitement. The characteristics of the earthquake that are considered are the scale factor, significant duration (D5-95 (s)), moment magnitude of the earthquake (magnitude), and Joyner-Boore distance (Rjb (km)).

2. 1. Buildings, Seismic Records, and Modeling

Dual RC (shear wall–frame) high-rise structures are adopted. The dual system buildings have 15, 20, 25, and 30 stories. The story height is equal to 3.5 m. The buildings plan consists of five bays (Figure 1). The gravity framing is considered using the leaning column, which is linked to the main structure. Rigid truss elements are used to connect the shear wall-steel frame and leaning columns and transfer the P-Delta effect. The design dead and live loads are $5kN/m^2$ and $2kN/$

m^2, respectively. The concrete compressive strength is assumed to be 55 MPa. Both longitudinal and transverse reinforcement has a yield strength of 420 MPa. In Appendix A, the fundamental parameters for material properties have been listed. The design was conducted based on ACI [23] and ASCE [24]. The building was also designed based on the modal response spectrum analysis (ASCE [24]), and the first 15 modes were used in the design. Table 1 presents the building site and the design parameters, which and are the maximum considered earthquake (MCE) spectral acceleration at short periods (S_s) and 1-s period (S_1), respectively. Table 2 provides the modal periods of the prototype buildings. Rayleigh damping is assumed. The damping is set as 2% of critical damping proportional to the mass and initial stiffness matrix. The dimensional details of the beams, columns and rebar sections of the concrete shear wall are presented in Appendix A.

The buildings' finite element model is generated by the OpenSees program [21,22] using displacement-based beam-column elements for the RC beams and columns. Concrete02 and Steel02 materials are used to define the material model of concrete and reinforcing steel fibers. The displacement-based beam-column element is a distributed-plasticity-fiber-based element based on Bernoulli's theory. Although different macro elements have been proposed for modeling concrete shear walls [25,26], in this study, RC walls are molded using a state-of-the-art element (SFI_MVLEM- Figure 2) and a nDMaterial FSAM material [26]. The SFI_MVLEM [26] element is a macro element which can simulate the behavior characteristics induced by non-linear shear deformation such as shear– axial/flexural interaction, shear cracking, stiffness deterioration, pinching effect, and strength deterioration. Studies have shown that (1) shear cracking can increase shear deformation of the walls in the plastic hinge region and (2) existing previous models usually underestimate compressive strains at the boundary elements, even for walls that their behavior is dominated by flexure. The confinement parameters of the boundary elements are calibrated according to the model proposed by Mander et al. [27].

TABLE 1. The building site and the design parameters

Latitude (degree)	Longitude (degree)	Design Cat.	Risk Cat.	Soil Cat.	S_s (MCE)	S_1 (MCE)
35.6535	-120.4407	D	I	D (stiff soil)	1.5g	0.6g

TABLE 2. The modal periods of the prototype buildings

Story	15	20	25	30
Modal periods (sec)	2.66	3.17	3.8	4.3

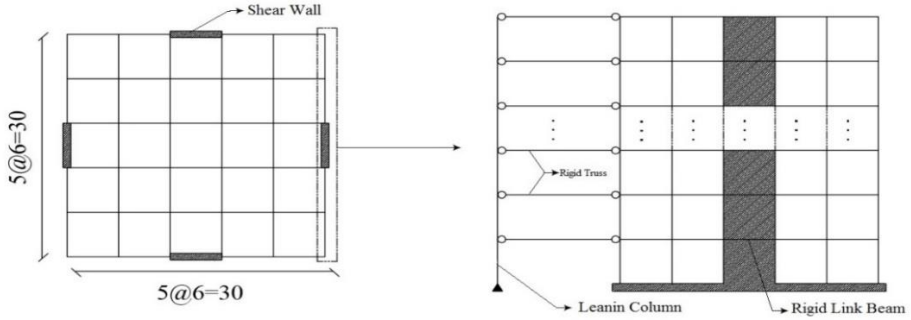

Figure 1. 2D model of the prototype buildings

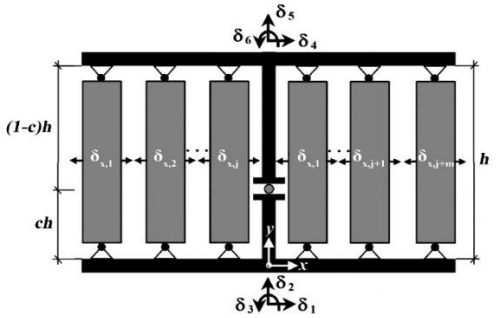

Figure 2. Shear-Flexure Interaction Multiple-Vertical-Line-Element Model (SFI-MVLEM).

The nonlinear time-history analyses are performed for the MCE level. The buildings are subjected to 150 seismic records, resulting in 600 non-linear response history analyses. Earthquake records are selected from the database of the Pacific Earthquake Engineering Research (PEER) center [28]. The key information of these records wall is presented in Appendix A. The minimum magnitude of records is taken as 6.0, and records are within a distance less than 20 km to the fault. Each ground motion is scaled in such a way that its response spectrum equals or exceeds the ASCE [24] spectrum over a determined period range (from 0.2T to

1.5T, where T is the first mode of vibration). All non-linear time-history analyses adopted the Newmark time integration method of constant acceleration. The Newton–Raphson iteration method is utilized to determine how the sequence of steps taken to solve the non-linear equation of motion. The convergence of the algorithm was based on the relative work increment. If a time step failed to converge, the Newton method switches to a modified Newton method with constant stiffness equal to the initial stiffness of the time step.

Model calibration is done using experimental results for reverse cyclic loading conducted by Tran and Wallace [29]. As an example, the element's response and related laboratory story test for specimen S78 are shown in Figure 3. Table 3 summarizes specimen information.

2. 2. Supervised Learning Methods One of the simplest supervised machine learning techniques is the family of regression models. Six regression models such as linear regression [30], Ridge regression [31], Lasso

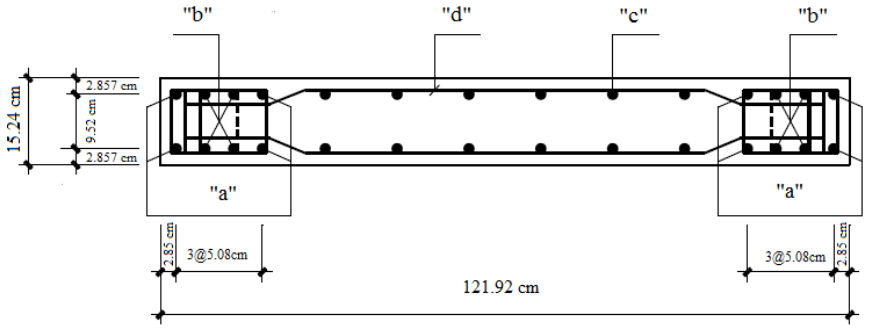

Specimen	a	b	c	d
S78	4#6	4#5	6#3 @ 0.127 m	#3 @ 0.127 m

b) Cross-section and reinforcement distribution

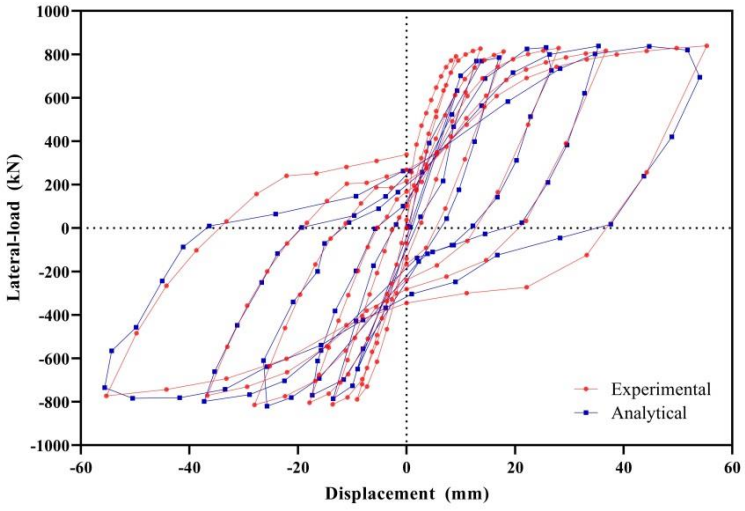

a) Global response

Figure 3. Typical cross-section and response for specimen S78.

TABLE 3. Specimen information

Aspect ratio	Web Reinf.	Boundary Reinf.	Compressive strength of concrete	Yield strengths of Reinf.
1.5	0.0073	0.0606	55 MPa	440-470 MPa

regression [32], Elastic net regression [33, 34], Huber regression [35], and RANSAC [36] are used in this paper. For further information on regression models, interested readers should study corresponding references of each model. In the case of the seismic demand model for the tall buildings, the input vector consists of the scale factor,

significant duration (D5-95 (s)), moment magnitude of the earthquake (magnitude), Joyner-Boore distance (Rjb (km)), and the maximum acceleration as well as velocity (Outputs from the non-linear time history analysis) in the tall building. . Significant duration (D5-95 (s)) is defined as the time needed to build up between 5 and 95 percent of the total Arias intensity for a specific earthquake record. The Joyner-Boore distance is defined as the shortest distance from a seismic station or any other site to the surface projection of the seismic event's rupture surface. Table 4 summarizes the range of parameters used. Other outputs from the non-linear time history analysis (the maximum base shear, maximum drift, and maximum displacement) are considered target variables.

Ordinary Least Square (OLS) regression (or linear regression) is one of the most widely known modeling techniques. The OLS regression is also known as linear regression. The OLS regression assumes that the relationship between the input variable (features vector,X) and the output variable (target vector,Y) is approximately linear (Equation (1)).

$$\hat{Y} = \beta^T X + \beta_0$$
$$\min_{\beta \in \mathbb{R}} \sum_{i=1}^{n} \|\beta^T x_i + \beta_0 - y_i\|^2 \quad (1)$$

where in Equation (1), $\hat{y}$is predicted values vector, $X = (x_1, x_2, \dots, x_i)$ are the n input variables,$Y = (y_1, y_2, \dots, y_i)$ are the n output variables, and β^T are the coefficients.

The OLS estimates often are subjected to the drawback of large variance. Previous studies have shown that there is a statistical trade-off between bias and variance. These observations have led to consider biased estimates such as Ridge regression. Ridge regression (Equation 2) introduces some bias by adding a penalty to the sum of the squared errors. Although model efficiency is decreased, the test error is decreased too. The coefficients are shrunk toward 0 as α becomes large.

$$\min_{\beta \in \mathbb{R}} \sum_{i=1}^{n} \|\beta^T x_i + \beta_0 - y_i\|^2 + \alpha \|\beta\|^2 \quad (2)$$

Note that in this case (using Ridge regression) solutions are not equivalent under scaling of the predictors (inputs); therefore, the predictors have to be standardized before using the Ridge regression model. The penalty contains the squared of the L2 norm of β (Equation (2)). The Lasso regression is a shrinkage method like Ridge regression. Lasso regression minimizes a loss function, using the L1 norm which is the sum of absolute values (Equation (3)).

$$\min_{\beta \in \mathbb{R}} \sum_{i=1}^{n} \|\beta^T x_i + \beta_0 - y_i\|^2 + \alpha \|\beta\|_1 \quad (3)$$

The difference between the L1 norm and L2 norm methods is that L1 penalizes coefficients equally but L2 penalizes more very large coefficients. In other words, for some values of α, L1 setting some coefficients equal to 0, and thus the most important variables are kept, this is called feature selection. Elastic Net is similar to Ridge regression and Lasso regression but uses both the L1 norm and L2 norm together (Equation (4)).

$$\min_{\beta \in \mathbb{R}} \sum_{i=1}^{n} \|\beta^T x_i + \beta_0 - y_i\|^2 + \alpha \cdot \eta \cdot \|\beta\|_1 + \alpha \cdot (1 - \eta) \cdot \|\beta\|_2^2 \quad (4)$$

where η is a coefficient that captures the relative amount of L1-penalty. This coefficient (η) is considered 0.5 [33, 34]. α needs to be determined by the analyst in Ridge, Elastic Net, and Lasso. By using the GridSearchCV in python, the value of α that maximizes the R^2 is calculated. The results are discussed further in section 3. In a sample, generally, outliers are considered as an example that differs remarkably from other observations. The models (Ridge, Elastic Net, and Lasso) are presented so far are sensitive to outliers since every single point participates in minimizing the function. To overcome this problem, Robust Regression is proposed. In the following, brief descriptions about Huber Regression and the RANdom SAmple Consensus (RANSAC), which allow the fit of robust regression, are provided. The Huber regression applies a piecewise function (loss) to samples that are classified as outliers. In other words, the loss optimizes either the squared loss or absolute loss for the samples based on a parameter (ε, Equation (5)). The cost function that Huber regression minimizes is given by:

$$\min_{\beta} \sum_{i=1}^{n} L(y_i, f(x_i))$$
$$where \quad (5)$$
$$L(y, f(x)) = \begin{cases} (y - f(x))^2 if |y - f(x)| < \varepsilon \\ 2 \cdot \varepsilon \cdot |y - f(x)| otherwise \end{cases}$$

Hence, the loss function is squared for small prediction errors. RANSAC is a non-deterministic algorithm that divides the complete data set into two different subsets (outlier and inlier). The inlier subset is also known as the hypothetical inliers which are used to fit the model. The basic steps of the RANSAC algorithm are summarized as follows: 1) Select randomly the minimum samples from the original data (the

TABLE 4. The modal periods of the prototype buildings

	Scale Factor	D5-95 (s)	Acc. ($\frac{m}{s^2}$)	Vel. ($\frac{m}{s}$)
Mean	8.43	23.63	7.33	1.37
Std.	9.11	12.24	2.81	0.57
Min.	0.47	7.2	1.52	0.39
25%	2.45	14.62	5.64	0.97
50%	5.68	20.6	6.95	1.27
75%	11.83	28.67	9.14	1.69
Max.	70.15	65.8	14.85	3.72

hypothetical inliers). 2) Fit a model to the selected points. 3) Points from the set of all points are then evaluated against the fitted model by considering a predefined tolerance. If the points fit the computed model well (using loss function), they will be considered as part of the consensus set (CS). 4) Save the estimated model as the best model if the consensus set is large enough ((the number of inliers/ the total number points) > predefined threshold). 5) Otherwise, repeat steps 1 through 4 (a trial and error process).

Although presented regression models provide remarkable feature selection, the prediction performance is limited. The main disadvantage of presented regression models is that they cannot consider non-linearity in the available data. An alternative method of tackling these problems is the use of Artificial Neural Networks. A neural network is a hierarchical organization of neurons which are joined by weighted connections. The structure of Artificial Neural Networks is made of three main components, which are referred to as (1) the input layer, which takes in a numerical representation of the data; (2) the hidden layer, where computations take place; and (3) the output layer. A direct consequence of this approach is an improvement of the estimation of drift, displacement, and base shear of different buildings. The network used to solve the problem in this study consists of three layers (input layer, one hidden layer, and output layer). We determined the number of neurons in the hidden layer and the percentage of the training and test data using a simulated annealing algorithm to reduce the computational time. Simulated Annealing (SA) is a stochastic algorithm for estimating the optimum value of a given function [37]. This method is inspired by the slow cooling of metals. The simulated annealing algorithm randomly selects a new potential solution. The range of the training dataset is 60-80% (X %) of the whole dataset, and the remaining ((100-X)/2 %) is used as the validation and test set. The codes are developed in MATLAB with its toolbox. The dataset (input and output) used in this section is the same as the regression models' dataset. A popular training algorithm (so-called "Trainlm" [37]) that updates weight and bias values according to Levenberg-Marquardt optimization is used. Activation functions for the hidden and output layers are hyperbolic tangent sigmoid (Tansig) and linear transfer function (Purelin), respectively.

2. 3. Simulated Annealing Algorithm Simulated annealing (SA) algorithm is one of the most preferred methods for solving optimization problems developed by Kirkpatrick et al. [39]. The SA algorithm, which is inspired by the slow cooling of metals, is a heuristic method with the basic idea of generating random displacement from any feasible solution. A probability function (Equation 6) is utilized to decide the transition between the current solution and the randomly generated new solution.

$$q = min\{1, e^{-\Delta E/K_B T}\} \quad (6)$$

where T is the control variable, q is the probability of accepting the potential solution, K_B is the Boltzmann constant, and ΔE is changes in the value of the objective function. The SA algorithm has some crucial advantages, including the following: (1) the SA algorithm is relatively easy to code, even for complex problems, and can deal with highly non-linear models, chaotic and noisy data, and many constraints.; (2) most optimization algorithms use the gradient descent, but the SA algorithm does not spend the computational time in calculating it; (3) the SA algorithm can be utilized to identify the minimum of the objective function more efficiently instead of being

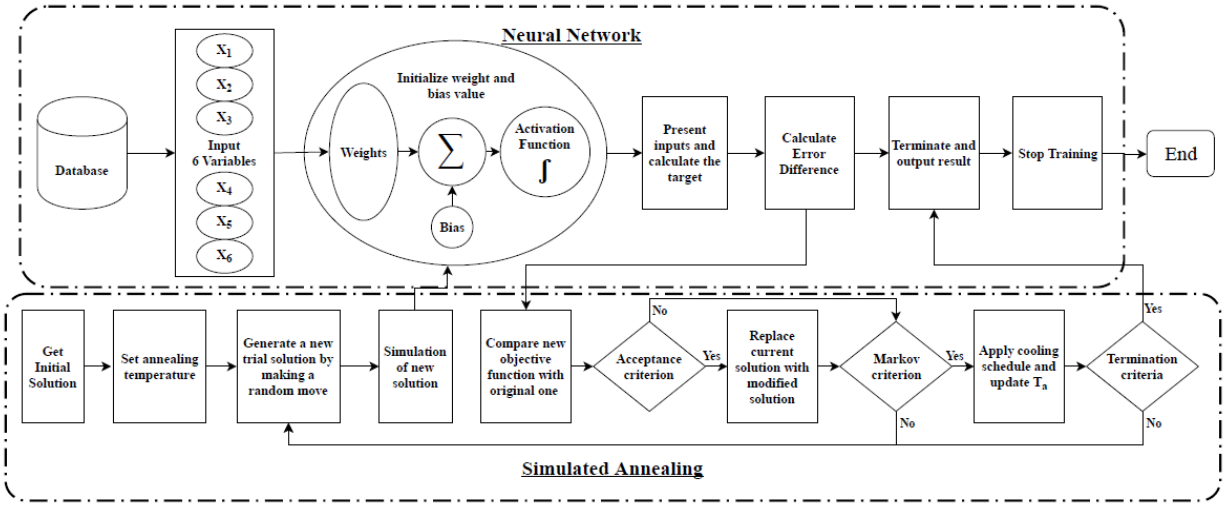

Figure 4. Computation procedure of the number of neurons and the percentage of the training and test data

trapped in a local minimum, and (4) Simulated annealing algorithm is independent of initial conditions [40]. As mentioned earlier, the number of neurons in the hidden layer and the percentage of the training and test data are determined using the simulated annealing algorithm. The proposed computation procedure of the number of neurons in the hidden layer and the percentage of the training data is summarized in the flow chart of Figure 4. The SA algorithm searches in the range 5-30 and 60-90% for the number of neurons in the hidden layer and the training data percentage, respectively.

3. RESULTS AND DISCUSSION

The machine learning techniques explained in the previous section are utilized to predict the high-rise concrete shear wall buildings' responses. The codes (regression models) are developed using a free software machine learning library of the Python programming language, so-called scikit-learn [41]. Observations (targets and features) are (randomly) split into two sets, traditionally called the test set and the training set. In this study, 80% and 20% of the entire dataset are considered for training and testing, respectively. The input variables are centered and scaled (a standard space with 0 mean and unit variance). Generally, the model is fitted on the training data, and the performance of the model is evaluated using unknown (test) data and the R^2 (Equation 7) or residual sum of squares (RSS, Equation 8) or mean square error (MSE, Equation 9) as score metric.

$$R^2 = 1 - \frac{\sum_i (y_i - \hat{y}_i)^2}{\sum_i (y_i - \bar{y})^2} \quad (7)$$

where $y_i$is the ith value of the variable to be predicted, $\bar{y}$is the average ofy_i, and $\hat{y}_i$predicted value ofy_i.

$$RSS = \sum_i (y_i - \hat{y}_i)^2 \quad (8)$$

$$MSE = \frac{1}{n}\sum_i (y_i - \hat{y}_i)^2 \quad (9)$$

The $R^2$is used in this study in order to compare the efficiency of the models in predicting the seismic demand (e.g., Table 5). The$R^2$is utilized because it is easily interpretable and it is a normalized version of the RSS. Besides, the R^2 does not depend on the scale of the data. The $R^2$is computed for the remaining data (test data).

In machine learning, a hyperparameter is a parameter whose value is utilized to control the learning process. As an example, the changes in the performance of the models (Elastic Net regression) against the changes in the hyperparameter α are shown in Figure 5. The performance of the models dramatically decreases as the hyperparameter α gets bigger. Based on these results, an optimum value of the hyperparameter α is chosen for each method and the target variable (displacement, drift, or base shear). The optimum value of the hyperparameter α is given in Appendix B. Here the performance of different methods utilized in this study is compared. Figure 6 (or Table 6) shows theR^2scores from 5 different regression models for displacement, drift, and base shear obtained using a test set for the different tall buildings. Overall Ridge, Lasso, Huber, and Elastic Net regression have very closeR^2scores for displacement, drift, and base shear. On the contrary, there is a difference between the RANSAC and other methods. The RANSAC regression performs the worst among the methods in estimating the base shear. Based on Figure 6, it can be concluded that the regression models have differentR^2scores for almost all the target variables and various buildings.

It is helpful to understand what factors may or may not impact estimating the tall building responses using regression methods. In order to compare regression coefficients, first, the average coefficients for all buildings are calculated for all target variables. Then, average coefficients are normalized by dividing each average coefficient by the sum of all the average coefficients to form a sum of 1.0. As an example, the process for displacement is shown in Figure 7.

TABLE 5. Results of Linear regression

Linear Reg.	Displacement	Drift	Base shear	Structure
R^2	0.65	0.70	0.65	15-stroy
R^2	0.7	0.70	0.65	20-story
R^2	0.6	0.65	0.69	25-story
R^2	0.72	0.75	0.77	30-story
Average	0.66	0.7	0.69	

TABLE 6. Results of Regression Models

Model	Structure		Displacement	Drift	Base-shear
Ridge	15-stroy	R^2	0.66	0.72	0.66
	20-story		0.72	0.72	0.65
	25-story		0.61	0.65	0.70
	30-story		0.73	0.75	0.78
	Average		0.68	0.71	0.69
Lasso	15-stroy	R^2	0.63	0.71	0.63
	20-story		0.76	0.75	0.69
	25-story		0.63	0.68	0.70
	30-story		0.73	0.77	0.75
	Average		0.69	0.73	0.69

Elastic Net	15-stroy	R^2	0.63	0.70	0.63
	20-story		0.74	0.75	0.69
	25-story		0.62	0.68	0.71
	30-story		0.71	0.77	0.76
	Average		0.68	0.73	0.70
Huber	15-stroy	R^2	0.64	0.73	0.65
	20-story		0.73	0.76	0.69
	25-story		0.63	0.68	0.70
	30-story		0.71	0.76	0.75
	Average		0.68	0.73	0.70
RANSAC	15-stroy	R^2	0.58	0.68	0.45
	20-story		0.65	0.72	0.51
	25-story		0.60	0.68	0.65
	30-story		0.73	0.79	0.82
	Average		0.64	0.72	0.61

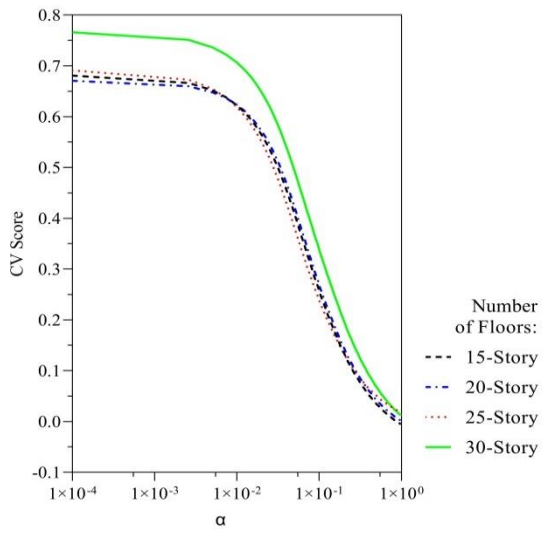

Figure 5. Elastic Net regression performance for predicting base shear of various structures

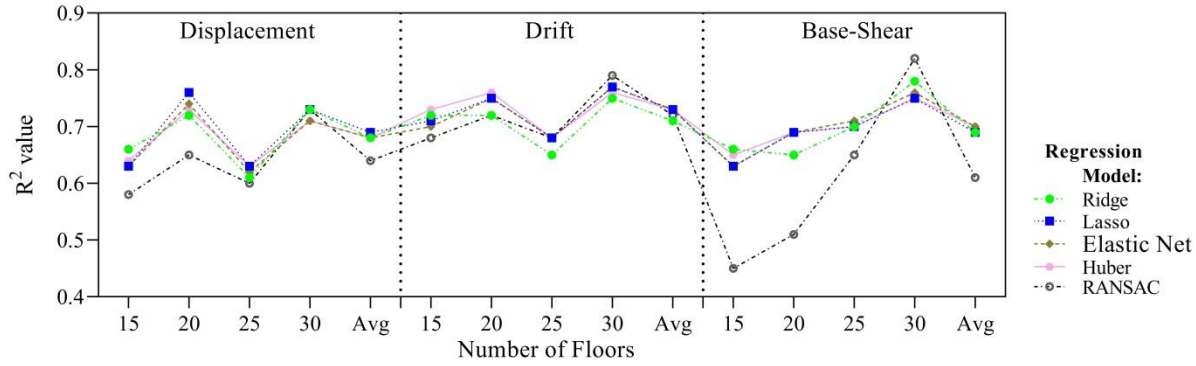

Figure 6. Results of Regression Models

Target	Scale Factor	5-95 Duration	Magnitude	Rjb	Acc.	Vel.	Structure
Displacement	x_{11}	x_{12}	x_{13}	x_{14}	x_{15}	x_{16}	15-story
	x_{21}	x_{22}	x_{23}	x_{24}	x_{25}	x_{26}	20-story
	x_{31}	x_{32}	x_{33}	x_{34}	x_{35}	x_{36}	25-story
	x_{41}	x_{42}	x_{43}	x_{44}	x_{45}	x_{46}	30-story
	$r_1=\frac{\sum_{i=1}^{4} x_{i1}}{4}$	$r_2=\frac{\sum_{i=1}^{4} x_{i2}}{4}$	$r_3=\frac{\sum_{i=1}^{4} x_{i3}}{4}$	$r_4=\frac{\sum_{i=1}^{4} x_{i4}}{4}$	$r_5=\frac{\sum_{i=1}^{4} x_{i5}}{4}$	$r_6=\frac{\sum_{i=1}^{4} x_{i6}}{4}$	average coefficient
	$r_1^N=\frac{r_1}{\sum_{i=1}^{6} r_j}$	$r_2^N=\frac{r_2}{\sum_{i=1}^{6} r_j}$	$r_3^N=\frac{r_3}{\sum_{i=1}^{6} r_j}$	$r_4^N=\frac{r_4}{\sum_{i=1}^{6} r_j}$	$r_5^N=\frac{r_5}{\sum_{i=1}^{6} r_j}$	$r_6^N=\frac{r_6}{\sum_{i=1}^{6} r_j}$	normalized coefficient

Figure 7. Results of Regression Models

Figure 8 shows the average-normalized estimated regression coefficients of various regression models for each target variable (displacement, drift, and base shear). Figure 8, the 0.0 values indicate that the associated features are not significant in predicting target variables. Also, Figure 8 illustrates that:

The crucial parameters to take into account tend to vary from method to method.

As mentioned above, the Elastic Net and Huber regression have the most R^2 scores, but unlike the first method, the second method recognizes more variables as influential input variables,

All regression models identify velocity as a significant input variable,

Huber and RANSAC regressions recognize all the input variables as influential variables,

In the case of displacement, all regression models identify velocity and magnitude as significant input variables,

In the case of base shear, all regression models identify velocity, acceleration, and magnitude as significant input variables,

Lasso, Ridge, and linear methods identify that the Rjb, 5-95 Duration, and scale factor have a minimal effect on predicting the target variable (seismic response).

In this study, the ANN-SA algorithm is utilized as an alternative solution. The Artificial Neural Network parameters are adjusted to maximize the R^2 to 1. Table 7 gives the number of neurons of the neural networks, which are determined using the simulated annealing algorithm for different buildings and target variables. Figure 9 depicts the results obtained from the ANN-SA algorithm. Comparison of the ANN-SA algorithm and regression results (Tables 6 and 7) reveals that the ANN-SA algorithm gives more accurate results for all predicted variables. Surely this could be due to the fact that the non-linearity of the relationship of the responses and features can be captured by an Artificial Neural Network. The above results emphasize the need for a comprehensive evaluation of different models before establishing a machine-learning-based response prediction model. Also, the percentage points of training, validation, and test data are determined using the simulated annealing algorithm. The results (Table 7) indicate that selecting the percentage points of training, validation, and test is an influential parameter.

The sensitivity analysis examines how uncertainty in a model's target variables can be apportioned to different uncertainty sources in the model input parameters. In other words, the sensitivity analysis allows the determination of the model key input factors of an output of interest. In this section, a MATLAB toolbox developed by Vu-Bac et al. [42] is used to carry out the sensitivity analysis. The framework links different steps from generating a sample, constructing the surrogate model, and implementing the sensitivity analysis method. The joint and conditional probability distribution functions of the input parameters are used to generate the

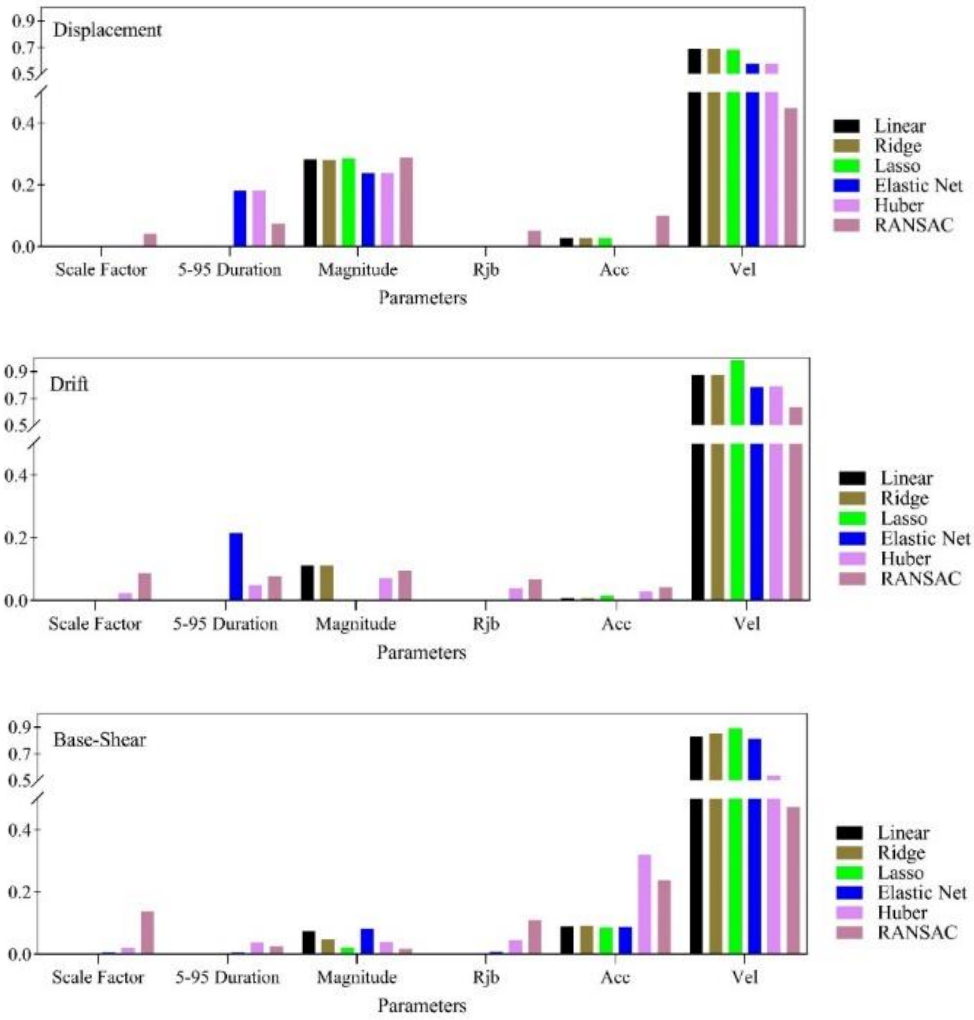

Figure 8. Average estimated coefficients for target variables

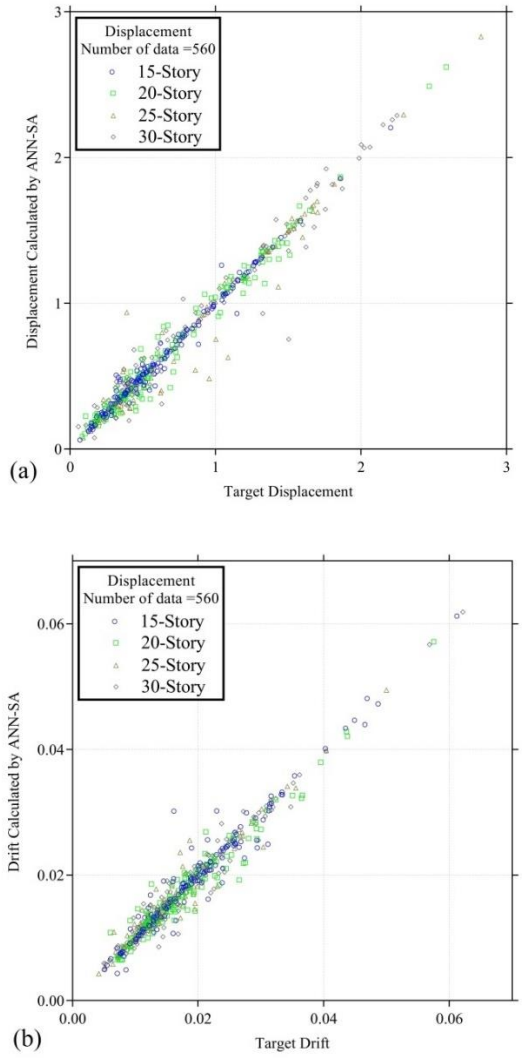

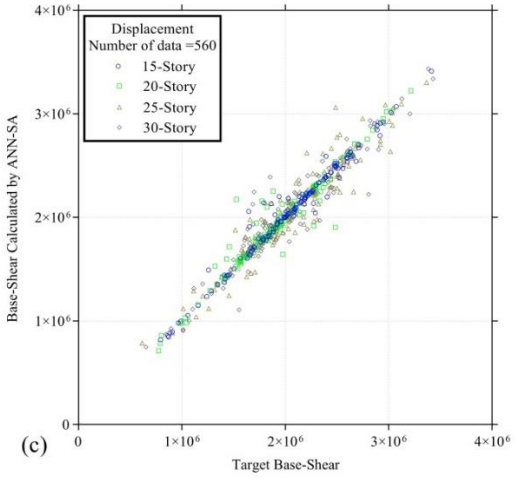

Figure 9. Performance of ANN-SA for estimating (a) Displacement (cm) (b) Drift (c) Base-Shear (N)

4. SENSITIVITY ANALYSIS

sample data since they must account for the input space constraints. The so-called surrogate-based approach is employed as an approximation of the real model for sensitivity analysis. The computation procedure of the sensitivity analysis is summarized in the flow chart of Figure 10. The description of the toolbox has been presented in literature [42]. Table 8 shows the results of the sensitivity analysis for all buildings. For all target variables (displacement, drift, and base shear), the earthquake's magnitude is estimated as the most crucial parameter. The second important parameter varies according to the building and the type of the target variable. Possible reasons for what may have caused this

TABLE 7. Results of Optimized Artificial Neural Networks

Story	Displacement			Drift			Base-shear		
	Neurons Num.	Training Percent	R^2	Neurons Num.	Training Percent	R^2	Neurons Num.	Training Percent	R^2
15	14	70	0.94	28	90	0.96	13	70	0.91
20	16	75	0.93	24	85	0.92	30	75	0.94
25	17	75	0.94	28	85	0.94	30	75	0.9
30	28	75	0.95	26	85	0.96	14	75	0.95
Average			0.94			0.94			0.92

issue can be: (1) structural responses are not identical since earthquake records have a random nature and their content are different from one another [43], and (2) as the building height increases, the effect of the modes (especially higher modes [44, 43]) on the structural response is increased, changing the structural behavior and response under a given earthquake.

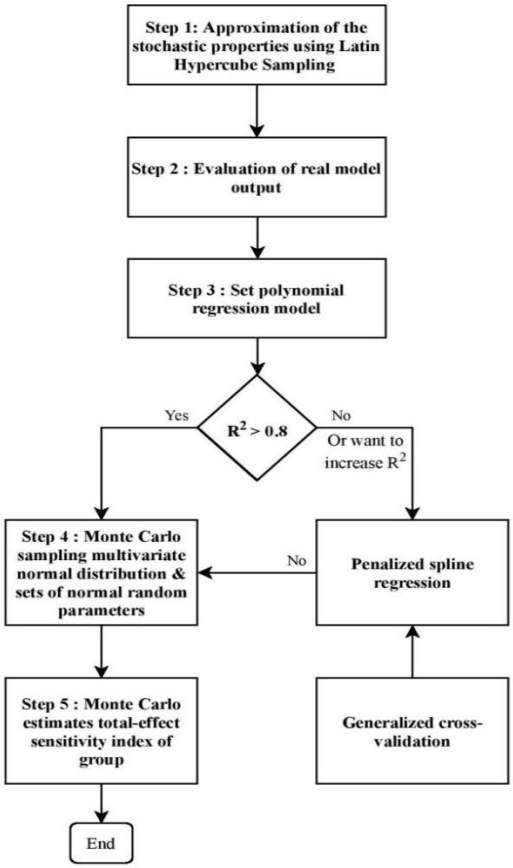

Figure 10. Diagram for sensitivity analysis

TABLE 8. Results of the sensitivity analysis for all buildings

15-story						
Target	**Scale Factor**	**Duration**	**Magnitude**	**Rjb**	**Acc.**	**Vel.**
Disp.	0.0004	0.0003	0.6661	0.0000	0.0012	0.0437
Drift	0.0031	0.0959	0.4580	0.0935	0.0312	0.0154
B. shear	0.0008	0.1668	0.3934	0.0091	0.0385	0.0440
20-story						
Target	**Scale Factor**	**Duration**	**Magnitude**	**Rjb**	**Acc.**	**Vel.**
Disp.	0.0000	0.0001	0.6769	0.0171	0.0020	0.0006
Drift	0.0036	0.0010	0.5450	0.0018	0.0021	0.0502
B. shear	0.0039	0.0009	0.4993	0.0004	0.0387	0.0097
25-story						
Target	**Scale Factor**	**Duration**	**Magnitude**	**Rjb**	**Acc.**	**Vel.**
Disp.	0.0000	0.0004	0.6764	0.0056	0.0001	0.0007
Drift	0.0016	0.0029	0.4438	0.0001	0.0003	0.0208
B. shear	0.0049	0.0379	0.1698	0.0019	0.0092	0.1429
30-story						
Target	**Scale Factor**	**Duration**	**Magnitude**	**Rjb**	**Acc.**	**Vel.**
Disp.	0	0	0.7268	0	0.0004	0.0016
Drift	0.0002	0.0065	0.6074	0.0001	0.0008	0.0304
B. shear	0.0004	0.0001	0.7296	0.0006	0.0153	0.0033

5. CONCLUSIONS

Reinforced concrete shear walls are used in high-rise buildings to resist earthquakes or wind loads. The need for an easy-to-use response estimation method for rapid damage assessment of the high-rise buildings after an earthquake leads to the study of existing simple regression methods and a hybrid technique, the Artificial Neural Network (ANN), and Simulated Annealing (SA) (ANN-SA model), for estimating the response of the structures in this study. In the initial part of this paper, four tall buildings were molded, and non-linear time-history analyses were performed to generate an extensive database. The computer software OpenSees was used to simulate the buildings under 150 earthquakes and calculate the responses. The primary purpose was to compare regression models and a standard Artificial Neural Network in predicting the tall building's response.

Analysis of results showed that if (1) during the earthquake, the maximum velocity created in the structure was stored (which can be done using the sensor) and (2) a database of the structure's responses to past earthquakes was produced (database) using existing software, the ANN-SA algorithm can use this information to estimate structural responses with acceptable accuracy.

Besides, the efficiency of different regression models such as RANSAC, Huber, linear, Ridge, Lasso, and Elastic Net regressions was studied in terms of estimation of structures' response. The training set (Eighty percent of the data) was utilized to fit the models, and the performance of the models was evaluated through the remaining unknown data (the test set). The performance of the regression models was assessed using scores. In general, the Elastic Net and Huber regression had better performance compared to other regression methods. Also, by using Ridge, Lasso, and Elastic Net regressions, the various input variables' relative importance on the estimated responses was identified. From the further exploration of the Elastic Net regression, critical parameters in determining the responses were velocity, acceleration, magnitude, and 5-95-Duration.

In order to evaluate the effect of non-linearity in the available data, the hybrid technique (ANN-SA algorithm) was utilized. The developed model had three-layer structures (input, hidden layer, and output layer). A simulated annealing algorithm was utilized to determine

the optimal number of the Artificial Neural Network neurons and the percentage of data that should be used in the training, validation, and testing set. By comparing the results of the ANN-SA algorithm and regression models, it can be concluded that (1) the effect of the non-linear relationship between data is significant, and considering it increases the accuracy of the model in predicting the target variables, and (2) the Artificial Neural Network outperforms regression models.

In addition, the sensitivity analysis was performed to examine how uncertainty in the target variables of a model could be apportioned to different sources of uncertainty in the model input parameters. The earthquake's magnitude was estimated as the most critical parameter, but the second important parameter varied according to the building and the type of target variable. Although the findings and conclusions are based on the case studies of four concrete shear wall buildings, the methodology has a wealth of applications in functional domains.

According to the literature and the results obtained in this study, it is suggested that researchers follow the process of the current paper for 3D modeling of irregular buildings and investigate the efficiency of Artificial Neural Networks for predicting their responses. Furthermore, the investigation of the Soil-Structure Interaction (SSI) effect can complement this research. Besides, comparing the performance of finite element and Neural Network models with the empirical vulnerability model of the actual seismic damage investigation can be very helpful and practical.

6. REFERENCES

1. Baltacıoğlu, A. K., Öztürk, B. A. K. İ., Civalek, Ö. M. E. R., Akgöz, B. E. K. İ. R. "Is Artificial Neural Network Suitable for Damage Level Determination of RC-Structures?" ***International Journal of Engineering and Applied Sciences***, Vol. 2, No. 3, (2010), 71-81.
2. Thaler, D., Stoffel, M., Markert, B., Bamer, F. "Machine-learning-enhanced tail end prediction of structural response statistics in earthquake engineering." ***Earthquake Engineering & Structural Dynamics***, (2021). https://doi.org/10.1002/eqe.3432
3. Goswami, S., Anitescu, C., Chakraborty, S., Rabczuk, T.: Transfer learning enhanced physics informed neural network for phase-field modeling of fracture, Theoretical and Applied Fracture Mechanics, 2020, 106, Article number 102447
4. H. Guo, X. Zhuang, and T. Rabczuk: A deep collocation method for the bending analysis of Kirchhoff plate. Computers, Materials and Continua, Vol. 59, No. 2, (2019), 433-456.
5. C. Anitescu, E. Atroshchenko, N. Alajlan, and T. Rabczuk: Artificial Neural Network methods for the solution of second order boundary value problems. Computers, Materials and Continua, Vol. 59, No. 1, (2019), 345-359.
6. Nguyen-Thanh, V.M., Zhuang, X., Rabczuk, T.: A deep energy method for finite deformation hyperelasticity, European Journal of Mechanics, A/Solids, 2020, 80, Article number 103874
7. Mangalathu, S., Jeon, J. S. "Classification of failure mode and prediction of shear strength for reinforced concrete beam-column joints using machine learning techniques." ***Engineering Structures***, Vol. 160, (2018), 85-94. https://doi.org/10.1016/j.engstruct.2018.01.008
8. Ebtehaj, I., Bonakdari, H., Es-haghi, M. S. "Design of a hybrid ANFIS–PSO model to estimate sediment transport in open channels." ***Iranian Journal of Science and Technology, Transactions of Civil Engineering***, Vol. 43, No. 4, (2019), 851-857. https://doi.org/10.1007/s40996-018-0218-9
9. Safari, M. J. S., Ebtehaj, I., Bonakdari, H., Es-haghi, M. S. "Sediment transport modeling in rigid boundary open channels using generalize structure of group method of data handling." ***Journal of Hydrology***, Vol. 577, (2019), 123951. https://doi.org/10.1016/j.jhydrol.2019.123951
10. Stoffel, M., Bamer, F., Markert, B. "Artificial Neural Networks and intelligent finite elements in non-linear structural mechanics." ***Thin-Walled Structures***, Vol. 131, (2018), 102-106. https://doi.org/10.1016/j.tws.2018.06.035
11. Sun, H., Burton, H. V., Huang, H. "Machine learning applications for building structural design and performance assessment: state-of-the-art review." ***Journal of Building Engineering***, (2020), 101816. https://doi.org/10.1016/j.jobe.2020.101816
12. Aydin, E., Öztürk, B., Guney, D. "Sensitivity analyses of variations on seismic response via viscous damper placement in planar building structures", ***10th International Conference on Urban Earthquake Engineering***, Tokyo, Japan, (Mar. 1-2, 2013), 2013.
13. Khaleghi, M., Salimi, J., Farhangi, V., Moradi, M. J., Karakouzian, M. "Application of Artificial Neural Network to Predict Load Bearing Capacity and Stiffness of Perforated Masonry Walls." ***Civil Engineering***, Vol. *2*, *No.* 1, (2021), 48-67. https://doi.org/10.3390/civileng2010004
14. Mangalathu, S., Jeon, J. S. "Machine learning–based failure mode recognition of circular reinforced concrete bridge columns: Comparative study." ***Journal of Structural Engineering***, Vol. 145, No. 10, (2019), 04019104. https://doi.org/10.1061/(ASCE)ST.1943-541X.0002402
15. Siam, A., Ezzeldin, M., El-Dakhakhni, W. "Machine learning algorithms for structural performance classifications and predictions: Application to reinforced masonry shear walls." ***Structures***, Vol. 22, (2019), 252-265. https://doi.org/10.1016/j.istruc.2019.06.017
16. Kiani, J., Camp, C., Pezeshk, S. "On the application of machine learning techniques to derive seismic fragility curves." ***Computers & Structures***, Vol. 218, (2019), 108-122. https://doi.org/10.1016/j.compstruc.2019.03.004
17. Gaba, A., Jana, A., Subramaniam, R., Agrawal, Y., Meleet, M. Analysis and Prediction of Earthquake Impact-a Machine Learning approach. 4th International Conference on Computational Systems and Information Technology for Sustainable Solution (CSITSS), Bengaluru, India, (2019). https://doi.org/10.1109/CSITSS47250.2019.9031026
18. Burton, H. V., Sreekumar, S., Sharma, M., Sun, H. "Estimating aftershock collapse vulnerability using mainshock intensity, structural response and physical damage indicators." ***Structural Safety***, Vol. 68, (2017), 85-96. https://doi.org/10.1016/j.strusafe.2017.05.009
19. Zhang, Y., Burton, H. V., Sun, H., Shokrabadi, M. "A machine learning framework for assessing post-earthquake structural safety" ***Structural Safety***, Vol. 72, (2018), 1-16. https://doi.org/10.1016/j.strusafe.2017.12.001
20. Zhang, Y., Burton, H. V. "Pattern recognition approach to assess the residual structural capacity of damaged tall buildings." ***Structural Safety***, Vol. 78, (2019), 12-22. https://doi.org/10.1016/j.strusafe.2018.12.004
21. Mazzoni S., McKenna F., Scott M. H., Fenves G. L. OpenSees command language manual. Pacific Earthquake Engineering Research (PEER) Center. 2006.

22. McKenna, F., Scott, M. H., Fenves, G. L. "Nonlinear finite-element analysis software architecture using object composition." ***Journal of Computing in Civil Engineering***, Vol. 24, No. 1, (2010), 95-107. https://doi.org/10.1061/(ASCE)CP.1943-5487.0000002
23. ACI A. 318-19. Building Code Requirements for Structural Concrete. ACI: Farmington Hills, MI, USA. 2019.
24. American Society for Civil Engineers (ASCE), "Minimum Design Loads and Associated Criteria for Buildings and Other Structures", ASCE/SEI 7-16, 2016. https://doi.org/10.1061/9780784414248
25. Barkhordari, M. S., Tehranizadeh, M., Scott, M. H. "Numerical modelling strategy for predicting the response of reinforced concrete walls using Timoshenko theory." ***Magazine of Concrete Research***, (2021), 1-23. https://doi.org/10.1680/jmacr.19.00542
26. Kolozvari, K., Orakcal, K., Wallace, J. W. "New opensees models for simulating nonlinear flexural and coupled shear-flexural behavior of RC walls and columns." ***Computers & Structures***, Vol. 196, (2018), 246-262. https://doi.org/10.1016/j.compstruc.2017.10.010
27. Mander J. B., Priestley M. J., Park R. "Theoretical stress-strain model for confined concrete." ***Journal of structural engineering***. Vol. 114, No. 8, (1988), 1804-26. https://doi.org/10.1061/(asce)0733-9445(1988)114:8(1804)
28. Ancheta T. D., Darragh R. B., Stewart J. P., Seyhan E., Silva W. J., Chiou B. S., Wooddell K. E., Graves R. W., Kottke A. R., Boore D. M., Kishida T. PEER 2013/03: PEER NGA-West2 Database. Pacific Earthquake Engineering Research. 2013.
29. Tran, T. A. "Experimental and analytical studies of moderate aspect ratio reinforced concrete structural walls." Doctoral dissertation, UCLA, (2012).
30. Hastie T., Tibshirani R., Friedman J. The elements of statistical learning: data mining, inference, and prediction. Springer Science & Business Media, (2009).
31. Hoerl A. E., Kennard R. W. "Ridge regression: Biased estimation for nonorthogonal problems." ***Technometrics***. Vol. 12, No. 1, (1970), 55-67. https://doi.org/10.1080/00401706.1970.10488634
32. Tibshirani R. "Regression shrinkage and selection via the lasso." ***Journal of the Royal Statistical Society: Series B (Methodological)***. Vol. 58, No. 1, (1996), 267-88. https://doi.org/10.1111/j.2517-6161.1996.tb02080.x
33. Zou H., Hastie T. "Regularization and variable selection via the elastic net." ***Journal of the Royal Statistical Society: Series B (Statistical Methodology)***. Vol. 67, No. 2, (2005), 301-20. https://doi.org/10.1111/j.1467-9868.2005.00503.x
34. Giussani A. Applied Machine Learning with Python. EGEA spa; 2020.
35. Huber P.J. Robust Estimation of a Location Parameter. In: Kotz S., Johnson N.L. (eds) Breakthroughs in Statistics. Springer Series in Statistics (Perspectives in Statistics). Springer, New York, NY, (1992). https://doi.org/10.1007/978-1-4612-4380-9_35
36. Fischler M. A., Bolles R.C. "Random sample consensus: a paradigm for model fitting with applications to image analysis and automated cartography." ***Communications of the ACM***, Vol. 24, No. 6, (1981), 381-395. https://doi.org/10.1145/358669.358692
37. Delgoshaei A., Rabczuk T., Ali A., Ariffin M. K. "An applicable method for modifying over-allocated multi-mode resource constraint schedules in the presence of preemptive resources." ***Annals of Operations Research***, Vol. 259, (2017), 85-117. https://doi.org/10.1007/s10479-016-2336-8
38. Scales L. E. Introduction to non-linear optimization. Macmillan International Higher Education; (1985). https://doi.org/10.1007/978-1-349-17741-7
39. Kirkpatrick S., Gelatt C. D., Vecchi M. P. "Optimization by simulated annealing." ***Science***, Vol. 220, (1983), 671-680. https://doi.org/10.1126/science.220.4598.671
40. Zain A. M, Haron H., Sharif S. "Genetic algorithm and simulated annealing to estimate optimal process parameters of the abrasive waterjet machining." ***Engineering with Computers***, Vol. 27, No. 3, (2011), 251-259. https://doi.org/10.1007/s00366-010-0195-5
41. Pedregosa F., Varoquaux G., Gramfort A., Michel V., Thirion B., Grisel O., Blondel M., Prettenhofer P., Weiss R., Dubourg V., Vanderplas J. "Scikit-learn: Machine learning in Python." ***Journal of Machine Learning Research***, Vol. 12, (2011), 2825-2830.
42. Vu-Bac N., Lahmer T., Zhuang X., Nguyen-Thoi T., Rabczuk T. "A software framework for probabilistic sensitivity analysis for computationally expensive models." ***Advances in Engineering Software***. Vol. 100, (2016), 19-31. https://doi.org/10.1016/j.advengsoft.2016.06.005
43. Chakroborty S., Roy R. "Role of ground motion characteristics on inelastic seismic response of irregular structures." ***Journal of Architectural Engineering***. Vol. 22, No. 1, (2016), B4015007. https://doi.org/10.1061/(asce)ae.1943-5568.0000185
44. Fatemi H., Paultre P., Lamarche C. P. "Experimental Evaluation of Inelastic Higher-Mode Effects on the Seismic Behavior of RC Structural Walls." ***Journal of Structural Engineering***, Vol. 146, No. 4, (2020), 04020016. https://doi.org/10.1061/(asce)st.1943-541x.0002509
45. Barkhordari, M. S., Tehranizadeh, M. "Ranking Passive Seismic Control Systems by Their Effectiveness in Reducing Responses of High-Rise Buildings with Concrete Shear Walls Using Multiple-Criteria Decision Making." ***International Journal of Engineering, Transactions B: Applications***, Vol. 33, No. 8, (2020), 1479-1490. https://doi.org/10.5829/ije.2020.33.08b.06

APPENDIX A

TABLE A1. Parameters of steel material

Yield strength	Initial elastic tangent	Strain-hardening ratio
$420MPa$	$200\ GPa$	0.01

TABLE A2. Parameters of concrete material

Compressive strength (MPa)	Unconf.	55
	Confined	66
Strain at the compressive strength	Unconf.	-0.002
	Confined	-0.005
Strain at the tensile strength	0.00008	
Tensile strength	$1.9MPa$	
Concrete modulus of elasticity	$37GPa$	

TABLE A3. The frame section of the buildings

Building	No. of story	Thickness (cm)	Long. Reinforcement
20-story	1-5	45	Ø25@15cm
	6-10	45	Ø20@20cm
	11-15	35	Ø20@25cm

	16-20	35	Ø20@25cm
25-story	1-5	45	Ø25@15cm
	6-10	45	Ø20@20cm
	11-15	45	Ø20@25cm
	16-20	35	Ø20@25cm
	21-25	35	Ø20@25cm
30-story	1-5	45	Ø25@15cm
	6-10	45	Ø20@20cm
	11-15	45	Ø20@20cm
	16-20	35	Ø20@25cm
	21-25	35	Ø20@25cm
	26-30	35	Ø20@25cm

TABLE A.4. List of ground motions

ID(s)	Name	Year	ID - Station Name
1-2	"Imperial Valley-06"	1979	1-"Brawley Airport" 2-"El Centro Array #10"
3-6	"Loma Prieta"	1989	3- "Gilroy - Historic Bldg." 4-"Gilroy Array #2" | 5-"Gilroy Array #3" | 6-"Saratoga - W Valley Coll." |
7	"Chi-Chi_ Taiwan"	1999	7-"CHY101"
8	"Duzce_ Turkey"	1999	8-"Bolu"
9	"Chuetsu-oki_ Japan"	2007	9- "Joetsu Kakizakiku Kakizaki"
10	"Darfield_ New Zealand"	2010	10- "Riccarton High School "
11-12	"El Mayor-Cucapah_ Mexico"	2010	11- "El Centro Array #12" 12- "Westside Elementary School"
13	"Imperial Valley-06"	1979	13- "El Centro Array #11"
14	"Superstition Hills-02"	1987	14- "Poe Road (temp)"
15	"Superstition Hills-02"	1987	15- "Westmorland Fire Sta"
16	"Northridge-01"	1994	16- "Beverly Hills - 14145 Mulhol"
17	"Kobe_ Japan"	1995	17- "Amagasaki"
18	"Kocaeli_ Turkey"	1999	18- "Duzce"
19	"Iwate_ Japan"	2008	19- "MYG005"
20-23	"El Mayor-Cucapah_ Mexico"	2010	20- "CERRO PRIETO GEOTHERMAL" 21- "MICHOACAN DE OCAMPO" | 22- "RIITO" | 23- "EJIDO SALTILLO" |
24	"Darfield_ New Zealand"	2010	24- "DFHS"
25	"Christchurch_ New Zealand"	2011	25- "Papanui High School "
26	"Northern Calif-03"	1954	26- "Ferndale City Hall"
27	"Coalinga-01"	1983	27- "Parkfield - Fault Zone 14"
28	"Loma Prieta"	1989	28- "Hollister - South & Pine" 29- "Hollister City Hall"
30	"Kobe_ Japan"	1995	30-"Sakai" 31- "Yae"
32-35	"Chi-Chi_ Taiwan"	1999	32- "TCU038" 33-"TCU112" | 34-"TCU117" | 35-"TCU118" |
36	"St Elias_ Alaska"	1979	36- "Icy Bay"
37	"Chi-Chi_ Taiwan-03"	1999	37-"CHY025" 38- "TCU065"
39	"Chuetsu-oki_ Japan"	2007	39- "Joetsu City"
40-42	"Iwate_ Japan"	2008	40- "Nakashinden Town" 41- "Semine Kurihara City" | 42- "Yokote Masuda Tamati Masu" |
43-47	"El Mayor-Cucapah_ Mexico"	2010	43- "TAMAULIPAS" 44-"El Centro - Meloland Geot. Array" | 45- "El Centro - Meloland Geotechnic" | 46-"El Centro Array #7" | 47- "El Centro - Meadows Union School" |
48-50	"Darfield_ New Zealand"	2010	48- "Hulverstone Drive Pumping Station" 49- "NNBS North New Brighton School " 50- "SPFS"
51	"Northwest Calif-02"	1941	"Ferndale City Hall"
52	"Northern Calif-01"	1941	"Ferndale City Hall"
53	"Borrego"	1942	"El Centro Array #9"
54	"Kern County"	1952	"Santa Barbara Courthouse"
55	"Kern County"	1952	"Taft Lincoln School"
56	"Southern Calif"	1952	"San Luis Obispo"
57	"Parkfield"	1966	"San Luis Obispo"
58	"Borrego Mtn"	1968	"El Centro Array #9"
59-75	"San Fernando"	1971	59- "2516 Via Tejon PV" 60-"Carbon Canyon Dam"

	61- "Cedar Springs Pumphouse" | 62- "Cedar Springs_ Allen Ranch" | 63- "Colton - So Cal Edison" | 64- "Fort Tejon" |		
	65-"Gormon - Oso Pump Plant" | 66- "LB - Terminal Island" | 67- "Pearblossom Pump" | 68- "Port Hueneme" | 69-"Puddingstone Dam (Abutment)" | 70- "Santa Anita Dam" | 71- "Tehachapi Pump" | 72- "Upland - San Antonio Dam" | 73- "Wheeler Ridge - Ground" | 74- "Whittier Narrows Dam" | 75- "Wrightwood - 6074 Park Dr" |		
76-78	"Friuli_ Italy-01"	1976	76- "Barcis" 77- "Codroipo" 78-"Conegliano"
79	"Tabas_ Iran"	1978	79-"Ferdows"
80-83	"Imperial Valley-06"	1979	80- "Coachella Canal #4"
	81- "Niland Fire Station" | 82-"Plaster City" | 83- "Victoria" |		
84	"Victoria_ Mexico"	1980	84- "SAHOP Casa Flores"
85-87	"Trinidad"	1980	85- "Rio Dell Overpass - FF"
	86- "Rio Dell Overpass_ E Ground" | 87- "Rio Dell Overpass_ W Ground" |		
88-91	"Irpinia_ Italy-01"	1980	88-"Arienzo"
	89-"Bovino" | 90-"Torre Del Greco" | 91-"Tricarico" |		
92-95	"Irpinia_ Italy-02"	1980	92- "Bovino"
	93-"Brienza" | 94- "Mercato San Severino" | 95- "Tricarico" |		
96-97	"Coalinga-01"	1983	96- "Parkfield - Cholame 12W" 97-"Parkfield - Cholame 1E"
98-126	"Coalinga-01"	1983	98-"Parkfield - Cholame 2E"
	99- "Parkfield - Cholame 2WA" | 100- "Parkfield - Cholame 3E" | 101- "Parkfield - Cholame 3W" | 102- "Parkfield - Cholame 4AW" | 103-"Parkfield - Cholame 4W" | 104- "Parkfield - Cholame 5W" | 105- "Parkfield - Cholame 6W" | 106- "Parkfield - Cholame 8W" | 107- "Parkfield - Fault Zone 1" | 108- "Parkfield - Fault Zone 10" | 109- "Parkfield - Fault Zone 2" | 110- "Parkfield - Fault Zone 3" | 111- "Parkfield - Fault Zone 4" | 112-"Parkfield - Fault Zone 6" |		
	113- "Parkfield - Fault Zone 9" | 114- "Parkfield - Gold Hill 1W" | 115-"Parkfield - Gold Hill 2E" | 116- "Parkfield - Gold Hill 2W" | 117-"Parkfield - Gold Hill 3W" | 118-"Parkfield - Gold Hill 4W" | 119- "Parkfield - Gold Hill 5W" | 120- "Parkfield - Gold Hill 6W" | 121-"Parkfield - Stone Corral 2E" | 122- "Parkfield - Stone Corral 3E" | 123-"Parkfield - Stone Corral 4E" | 124- "Parkfield - Vineyard Cany 3W" | 125- "Parkfield - Vineyard Cany 4W" | 126-"Parkfield - Vineyard Cany 6W" |		
127	"Ierissos_ Greece"	1983	127- "Ierissos"
128-136	"Taiwan SMART1(25)"	1983	128-"SMART1 C00"
	129-"SMART1 E01" | 130- "SMART1 E02" | 131- "SMART1 I01" | 132- "SMART1 I07" | 133- "SMART1 M01" | 134-"SMART1 M06" | 135- "SMART1 O01" |		
	136- "SMART1 O07" |		
137-143	"Borah Peak_ ID-01"	1983	137- "CPP-601" 138-"CPP-610"
	139- "PBF (second bsmt)" | 140-"TAN-719" | 141- "TRA-642 ETR Reactor Bldg(Bsmt)" | 142- "TRA-670 ATR Reactor Bldg(Bsmt)" |		
143-150	"Morgan Hill"	1984	143- "APEEL 1E - Hayward"
	144- "Capitola" | 145- "Foster City - APEEL 1" | 146-"Fremont - Mission San Jose" | 147- "Hollister City Hall" |		
	148- "Los Banos" | 149-"SF Intern. Airport" | 150- "San Justo Dam (L Abut)" |		

APPENDIX B

TABLE B1. Comparison of α (Ridge Reg.)

Ridge Reg.	Displacement	Drift	Base shear	Structure
α	0.001	0.022	0.022	15-stroy
α	0.001	0.278	0.278	20-story
α	0.001	0.022	0.022	25-story
α	0.001	0.002	0.001	30-story

TABLE B2. Comparison of α (Elastic Net Reg.)

Elastic Net Reg.	Displacement	Drift	Base shear	Structure
α	0.01326	0.00130	0.2222	15-stroy
α	0.02811	0.00010	0.2222	20-story
α	0.04941	0.00167	0.0193	25-story
α	0.01900	0.00115	0.1264	30-story

TABLE B3. Comparison of α (Lasso Reg.)

Lasso Reg.	Displacement	Drift	Base shear	Structure
α	0.00052	0.00010	1526.41	15-stroy
α	0.00168	0.00010	2223.00	20-story
α	0.00268	0.00010	3237.45	25-story
α	0.00066	0.00010	3237.46	30-story

Persian Abstract

چکیده

پیش بینی پاسخ‌های دیوارهای برشی بتن آرمه تحت اثر حرکات قوی زمین در طراحی، ارزیابی و تصمیم گیری راهبردهای مقاوم سازی بسیار مهم است. این مطالعه توانایی مدل‌های رگرسیون و یک روش ترکیبی (مدل ANN-SA)، شبکه عصبی مصنوعی (ANN) و الگوریتم تبرید شبیه‌سازی‌شده (SA)، را برای پیش بینی پاسخ دیوارهای برشی بتن آرمه تحت تأثیر حرکت‌های قوی زمین ارزیابی می‌کند. برای این منظور، چهار ساختمان (۱۵ ، ۲۰ ، ۲۵ و ۳۰ طبقه) با دیوارهای برشی بتنی در OpenSees مورد تجزیه و تحلیل قرار گرفته است. ۱۵۰ رکورد لرزه ای برای تولید یک پایگاه داده جامع از ورودی (مشخصات) و خروجی (پاسخ ها) مورد استفاده قرار گرفته است. حداکثر شتاب، حداکثر سرعت و مشخصات زلزله به عنوان پیش بینی کننده (متغییرهای ورودی) استفاده شده است. در این مطالعه دقت مدل های ساده و روش ترکیبی در شناسایی پاسخ‌های دیوارهای برشی مقایسه شده و همچنین حساسیت متغیرهای ورودی به مدل تقاضای لرزه‌ای بررسی شده است. نتایج نشان می‌دهد که مدل ANN-SA از دقت منطقی در پیش بینی برخوردار است.